

# Blood flow imaging of thyroid and carotid artery using singular value decomposition filter

特異値分解フィルタを用いた甲状腺および頸動脈の血流イメージング

Hayato Ikeda<sup>1†</sup>, Takuro Ishii<sup>2</sup>, and Yoshifumi Saijo<sup>3</sup> (<sup>1</sup>Tohoku Univ. Graduate School of Biomedical Engineering; <sup>2</sup>Frontier Research Institute for Interdisciplinary Sciences;)

池田 隼人<sup>†</sup>, 石井 琢郎<sup>2</sup>, 西條 芳文<sup>3</sup>

(<sup>1</sup>東北大学大学院医工学研究科, <sup>2</sup>東北大学学際科学フロンティア研究所)

## 1. Introduction

Ultrafast ultrasonic imaging based on plane or diverging waves transmissions can acquire rich two-dimensional blood flow signals at very high frame rates. To visualize the blood flow signal clearly, the singular value decomposition (SVD) filter is applied to effectively suppress tissue clutter signal using differences in spatiotemporal characteristics and signal amplitude, and is known to outperform conventional clutter filters, i.e., high-pass temporal filtering in the removal performance of tissue signals<sup>1-2</sup>). In order to improve the accuracy of blood flow detection, this study investigated the performance of the SVD filter using the periodicity of beats with a larger ensemble size. The proposed method was validated by in vivo measurement of the carotid artery and thyroid.

## 2. Materials and Methods

### 2.1 Experimental set up

A liner array ultrasound probe with a center frequency of 7.6 MHz (Verasonics Inc, L11-5v) was connected to a programable ultrasound scanner (Verasonics Vantage 256) to acquire RF data for ultrasound ultrasonic imaging. Carotid artery and thyroid were imaged in order to acquire ultrasonic data of beating tissue and blood flow.

### 2.2 Acquisition of signals

**Fig.1** shows a schematic of the sequence of ultrafast ultrasound imaging. Plane waves were transmitted at a PRF of 5.0 kHz at steering angles of -9, -4.5, 0, 4.5, 9 degrees for compounding operation. Hence, the frame rate of imaging was 1.0 kHz. Image data can be expressed as a complex variable  $\mathbf{S}(z, x, t)$ , which is an analytical signal at a spatial position (depth  $z$ , lateral dimension  $x$ ) in a frame at time  $t$ . In this paper, the analytical data were named IQ data. The IQ data of 2000 frames (= 2.0 s) were acquired for pulsatile flow imaging. The size of the IQ data  $\mathbf{S}(z, x, t)$  was 300 pixels  $\times$  128 pixels  $\times$  2000 pixels ( $n_z \times n_x \times n_t$ ).

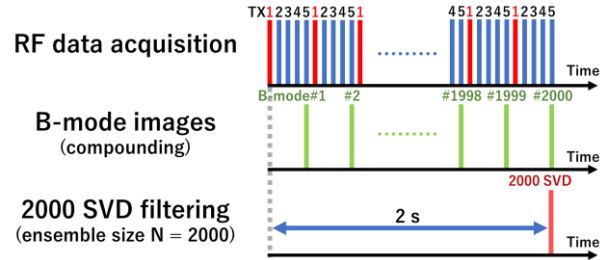


Fig. 1 Sequence of ultrafast ultrasound imaging.

### 2.3 Singular value decomposition

Three-dimensional data  $\mathbf{S}(z, x, t)$  were rearranged as two-dimensional data  $\mathbf{M}(m, n)$ , where  $m$  and  $n$  are the numbers of a column and a row, respectively. The covariance matrix  $\mathbf{C}_M(n, n)$  of  $\mathbf{M}(m, n)$  is presented here in magnitude and is of dimension  $n_t \times n_t$  as expressed in **Eq.1**,

$$\mathbf{C}_M(i, j) = \frac{1}{n_m n_n} \sum_{m \cdot n} (|\mathbf{M}_i| - \langle |\mathbf{M}_i| \rangle) \times (|\mathbf{M}_j| - \langle |\mathbf{M}_j| \rangle). \quad (1)$$

The value of  $\mathbf{C}_M(n, n)$  fluctuates according to the pulsation cycle. SVD of the matrix  $\mathbf{M}(m, n)$  provides a diagonal matrix  $\Delta$  containing singular values  $\lambda_i$ , unitary matrix  $\mathbf{U}(m, m)$  of spatial singular vectors, and unitary matrix  $\mathbf{V}(n, n)$  of temporal singular vectors as expressed in **Eq.2**,

$$\mathbf{M}(m, n) = \mathbf{U} \cdot \Delta \cdot \mathbf{V}^*. \quad (2)$$

The singular values  $\lambda_i$  are arranged from the most energetic to the least ( $\lambda_1 \rightarrow \lambda_{2000}$ ). Boundary singular vector numbers  $\#p$  was chosen to obtain SVD-filtered blood flow signals  $\mathbf{S}_{blood}(z, x, t)$  and its power integral  $\mathbf{PW}(z, x)$  as expressed in **Eq.(3)** and **Eq.(4)**,

$$\mathbf{S}_{blood}(z, x, t) = \sum_{i=p}^{2000} \lambda_i \cdot \mathbf{U}_i(z, x) \cdot \mathbf{V}_i(t), \quad (3)$$

$$\mathbf{PW}(z, x) = \int |\mathbf{S}_{blood}(z, x, t)|^2 dt, \quad (4)$$

where  $\mathbf{U}_i$  and  $\mathbf{V}_i$  are the  $i^{\text{th}}$  columns of  $\mathbf{U}$  and  $\mathbf{V}$ , respectively. The choice of  $\#p$  to determine the boundary between the tissue and the blood flow signal is achieved by using the covariance matrix of spatial singular matrix  $\mathbf{U}^3$ .

### 3. Result and Discussion

**Fig.2** shows B-mode images of carotid artery and thyroid, and covariance matrix of B-mode images from 1 to 2000 frame. It was confirmed that the value of the covariance matrix changed with the pulsation cycle.

**Fig.3** shows set of spatiotemporal singular vectors of carotid artery (a) #2-#200, (b) #200-2000, (c) #1980-#2000. The spatial singular vectors correspond to the spatial information of each signal, and the temporal singular vectors correspond to the temporal change between frames. The spatial distribution of the blood vessel wall (#2-200) has a temporal change with pulsation. The signal intensity of the spatial distribution of blood flow (#200-2000) decreases at the timing of beating. In the other hand, the blood flow signal component contained in noise (#1980-#2000) increases. In other words, the blood flow component shifts to the higher-order side of the singular value during beating.

**Fig.4** shows set of spatiotemporal singular vectors of thyroid (a) #2-#150, (b) #150-2000, (c) #1980-#2000. Even in the thyroid gland, which is less affected by pulsation than the carotid artery, it was confirmed that the spatial distribution of blood flow decreased at the time of pulsation.

**Fig.5** shows Power doppler images of blood flow of carotid artery and thyroid, respectively. Noise depending on the depth direction could be confirmed.

### 4. Conclusion

In this study, the SVD filter using the periodicity of beats with larger ensemble size was proposed to apply detecting blood vessel beating and blood flow selectively. The proposed method was verified by in vivo measurement of the carotid artery and thyroid.

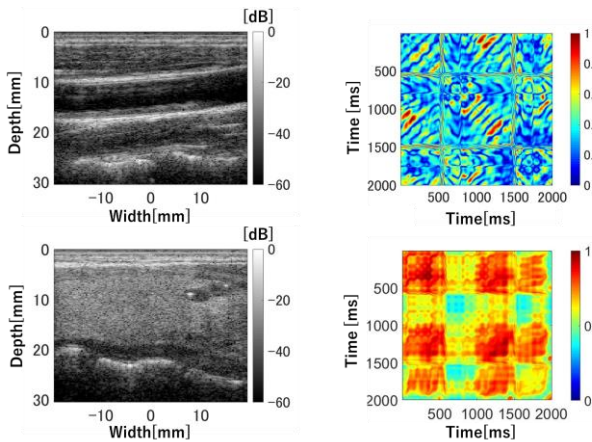


Fig. 2 B-mode images of carotid artery and thyroid, and covariance matrix of B-mode images from 1 to 2000 frame.

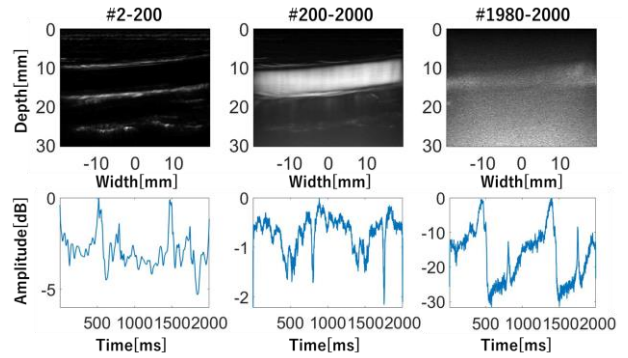


Fig. 3 Set of spatiotemporal singular value vectors of carotid artery.

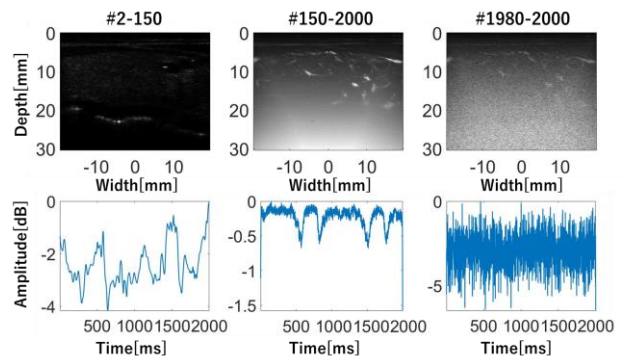


Fig. 4 Set of spatiotemporal singular value vectors of thyroid.

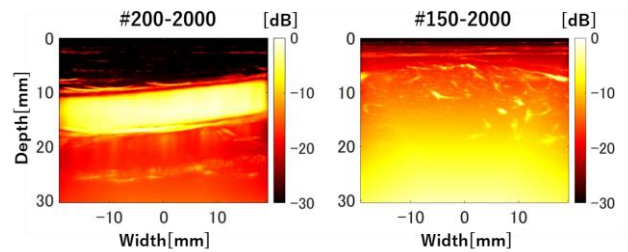


Fig. 5 Power doppler images of blood flow of carotid artery and thyroid, respectively.

### Acknowledgment

This work was supported by a Grant-in-Aid for JSPS Research Fellow, 20J11155.

### References

1. C. Demené, T. Deffieux and M. Tanter: IEEE Trans. Med. Imaging **34**, 2271 (2015).
2. B. Arnal, J. Baranger and M. Pernot: Phys. Med Biol. **62**, 843 (2017).
3. J. Baranger, B. Arnal and C. Demene: IEEE Trans. Med. Imaging **37**, 1574 (2018)